Journal of Nuclear Materials 595 (2024) 155046

Contents lists available at ScienceDirect

Journal of Nuclear Materials

journal homepage: www.elsevier.com/locate/jnucmat

Short communication

The lattice contraction of UO_2 from Cr doping as determined via high resolution synchrotron X-ray powder diffraction

Gabriel L. Murphy [a,*], Volodymyr Svitlyk [b,c], Maximilian Henkes [a], Daniil Shirokiy [a], Christoph Hennig [b,c], Philip Kegler [a], Dirk Bosbach [a], Andrey Bukaemskiy [a]

[a] Institute of Energy and Climate Research (IEK-6), Forschungszentrum Jülich GmbH, Jülich 52428, Germany
[b] Institute of Resource Ecology, Helmholtz Zentrum Dresden-Rossendorf, Dresden 01328, Germany
[c] The Rossendorf Beamline at ESRF, The European Synchrotron, CS40220, Grenoble CEDEX 9 38043, France

ARTICLE INFO

Keywords:
Diffraction
Rietveld
Synchrotron
Cr-doped UO_2
X-ray
Nuclear fuel

ABSTRACT

High resolution synchrotron powder X-ray diffraction analysis of Cr-doped UO_2 samples with additions of Cr_2O_3 as 0, 500, 1000, 1500, 2500 to 3500 ppm prepared under sintering conditions of -420 kJ/mol and 1700 °C is reported. The lattice dependence from Cr doping is established through the Rietveld refinement method where the rate of linear lattice parameter contraction from Cr doping, Δa_{cr}, was found to be considerably smaller and more subtle than previously described. This investigation highlights the need for high resolution and precise specimen preparation when measuring and interpreting subtle changes to nuclear material crystal structures due to trace doping.

1. Introduction

Cr-doped UO_2 is used commonly as a part of modern nuclear fuel blends due its ameliorated properties over classical non-doped UO_2, where it has been deployed in both North American and European power reactor units [1]. The addition of chromia (Cr_2O_3) during fuel fabrication results in enhanced grain growth that enables improved fission gas retention and fuel density leading to improved thermal conductivity allowing the fuel to be used at higher burn ups [2]. Chemically, the addition of Cr into UO_2 is a complex process where the combination of the small size Cr^{+3} cation compared to U^{+4} coupled with the variable behaviour at sintering temperatures results in only ppm level solubility of Cr in the UO_2 matrix. This is further exacerbated by the formation of a variety of secondary phases [3–7], including eutectic compositions, whilst precise Cr addition control often suffers from volatilisation effects during sintering [8]. The formation of eutectic compositions in addition to the lattice matrix incorporation of Cr is understood to be the leading cause of improved grain growth in the material [6,9]. The solubility of Cr in UO_2 is further highly dependent on the specific conditions used during sintering, specifically the oxygen partial pressure (μ_{O2}) and temperature applied. Under an μ_{O2} and temperature of -420 kJ/mol and 1700 °C respectively the solubility of Cr in UO_2 is understood to be 750 ppm as Cr [3,6]. Higher solubilities can be obtained towards 1000 ppm Cr via higher temperatures and increased μ_{O2} [10]. Consequently, this results in only a subtle contraction of the UO_2 fluorite structure as Cr is incorporated into it progressively [10,11]. The incorporation of Cr into UO_2 was recently determined via high resolution spectroscopic methods of single crystal grains and bulk material to follow the mechanism $(Cr_x^{+3}U_{1-x}^{+4})O_{2-0.5x}$ that had been subject to strong debate prior, with the additional formation of oxide and metallic phases including Cr^0, Cr^{+2} and $Cr_2^{+3}O_3$ [3]. The relevant abundance and distribution of these phases was found to be consistent and corroborate previous thermodynamic estimates of Cr-doped UO_2 [6].

Although good progress has been made in the determination of the Cr-doped UO_2 redox chemistry, disagreement remains regarding the lattice parameter as Cr is progressively incorporated into the UO_2 fluorite structure and the associated rate of contraction. The contraction has been frequently used to indirectly monitor the content of Cr in UO_2 in addition to inferring chemistry of Cr in UO_2 [11,12]. However, when literature values are considered, a wide variation of lattice parameters are reported [10,11,13], which appears to have contributed to disagreement over redox determination of Cr in the UO_2 lattice [6,11,12]. Critically, inspection of these values shows that these previous studies have all been conducted using standard laboratory X-ray powder

* Corresponding author.
E-mail address: g.murphy@fz-juelich.de (G.L. Murphy).

https://doi.org/10.1016/j.jnucmat.2024.155046
Received 2 February 2024; Received in revised form 8 March 2024; Accepted 20 March 2024
Available online 21 March 2024

diffraction often on pellet samples rather than fine powders. Although such devices provide well for rudimentary sample characterisation, the described subtle shift in lattice parameter from Cr incorporation into UO_2 can be difficult to precisely track due effects arising from instrument related peak width broadening, asymmetry and Kα2 components (when a Cu X-ray source is used) in addition to sample related effects such as displacement, transparency or surface roughness in the case of pellets. These effects complicate accurate determination of Bragg positions and require careful corrections to ensure accurate and precise measurement, particularly on pellet samples [14,15], in order to ascertain correct and meaningful chemical and structural interpretations.

To precisely resolve accurate and precise changes to lattice parameters, high resolution methods are necessary in which synchrotron X-ray powder diffraction is often considered the gold standard owing to superior brilliance of the beam source often combined with state-of-the-art detection equipment, which often exceeds that of standard laboratory X-ray tube-based methods. Interestingly, there does not appear to be any reported studies on Cr-doped UO_2 utilising high resolution diffraction, despite many successful applications of it to many other actinide oxides [16–19]. Accordingly, in order to precisely determine the lattice contraction of UO_2 as Cr is incorporated progressively into it, the present investigation has used high resolution synchrotron X-ray diffraction measurements to examine fine powders of Cr-doped UO_2 samples with additions of Cr at 0, 500, 1000, 1500, 2500 to 3500 ppm additions of Cr (as Cr_2O_3) where each sample was prepared using consistent sintering conditions of -420 kJ/mol and 1700 °C. Collected diffractograms were analyzed using the Rietveld refinement method where the precise structural dependence of the UO_2 contraction from Cr doping was established. These results are discussed in detail together with other related investigations of the lattice parameter contraction Cr doping in UO_2, with particular regard to type of measurement performed and resolution.

Cr-doped UO_2 ceramics with 0, 500, 1000, 1500, 2500 and 3500 ppm additions of Cr (as Cr_2O_3) were generated using a co-precipitation method beginning with doped ammonium diuranate (ADU) based on a previously established method [7]. The doped ADU was prepared using stoichiometrically controlled amounts of uranyl nitrate ($UO_2(NO_3)_2$) and chromium nitrate ($Cr(NO_3)_3$) that were mixed in solution, followed by precipitation using ammonia (NH_3) involving a 300 % excess. Samples with targeted 0, 500, 1000, 1500, 2500 and 3500 ppm additions of Cr (as Cr_2O_3) (0, 342, 684, 1026, 1711 and 2395 ppm respectively as Cr elemental) were generated via this method. The ADU mixtures were firstly calcined under air to oxide form using a box furnace at 800 °C for 5 h prior to reduction to UO_2 at 600 °C under 4 % H_2–96 % Ar atmosphere for additional 5 h. In both steps the samples were in powder form. Finally, the pre-treated powders were compacted into pellets and heated to 1700 °C using a tube furnace for 10 h with a μ_{O2} of -420 kJ/mol that was monitored and produced via a 4 % H_2–96 % Ar and 1 % O_2–99 % Ar gas mixture. The furnace was cooled to room temperature using a ramp rate of 6 °C/min whilst the gas mixture was maintained.

Ambient temperature synchrotron X-ray powder diffraction (S-XRD) experiments were performed at the BM20 Rossendorf beamline [20] (ROBL) at the European Synchrotron Radiation Facility (ESRF), Grenoble, France. Diffraction data were collected on high-resolution XRD1 machine equipped with a Dectris Eiger CdTe 500k photon counting detector at 23 °C. Synthesised samples were finely ground and packed in glass capillaries of 0.3 mm diameter enclosed in 1 mm Kapton tubes that serve as confinement barriers. The monochromator energy was calibrated against the K-edge X-ray absorption spectrum of a yttrium metal foil using the first inflection point at 17 038 eV which provides an uncertainty of ± 0.3 eV (± 0.000013 Å). The energy was then shifted and set to 16 000 eV and detector geometry of the experimental setup was calibrated using silver behenate and a LaB_6 NIST standard reference. The wavelength was subsequently determined to be 0.7749 Å. Experiments were performed in transmission mode at 23 °C and corresponding 2D data were reduced using the PyFAI library adapted for diffractometers mounted on a goniometer arm [21]. Structural analysis was performed using the Rietveld method as implemented in the program GSAS-II [22]. The peak shapes were modelled using a pseudo-Voigt function and the background was estimated using a 6–12 term shifted Chebyschev function. The scale factor, absorption detector zero-point and lattice parameters were refined together with the peak profile parameters.

2. Results

Precise determination of the lattice parameters for studied compositions was made using the Rietveld refinement method in which fluorite structures in space group $Fm\bar{3}m$ were refined against each of collected S-XRD data sets. Inspection of the diffraction patterns indicated contraction of the fluorite structure as evident by shifting of Bragg reflections to higher 2θ but only subtly. The Rietveld profiles for each collected sample are provided in Fig. 1 and determined lattice parameters are given in Table 1. The lattice parameter for the as measured UO_2 sample was determined to be 5.46894(2) Å which is slightly smaller than that reported by Leinders et al. [23] at 5.47127(8) Å, nevertheless, the value is considered acceptable and consistent with other previous studies. Attempts were made to perform the Rietveld refinements with Cr in the structural model corresponding to the expected amount in the lattice based on the amount of Cr addition and considering the Cr phase distribution given by recent spectroscopic phase analysis [24] thermodynamic modelling [6] and volatility studies of Cr-doped UO_2 [8]. From this, the maximum occupancy of Cr on the U position is 0.01. However it was found that no significantly meaningful improvement of the refinement could be obtained.

The determined lattice parameters from S-XRD measurements provided in Table 1 are plotted as a function of Cr content in Fig. 2a with previous literature values from Leenaers et al. [10], Kegler et al. [7], Cardinaels et al. [11] and Milena-Pérez et al. [13] who all studied Cr-doped UO_2 but used laboratory XRD methods all using pellet measurements [7,10,11,13]. The normalized lattice parameter (a/a_o) is additionally plotted in Fig. 2b with described reference values.

Apparent from Fig. 2a is the relatively large spread of lattice parameter values reported from different studies for Cr-doped UO_2 as a function of Cr doping. Notably all other investigations used laboratory XRD and particularly measured pellet samples rather than fine powders. Specific conditions used during synthesis would affect uptake of Cr into the UO_2 lattice matrix, which in turn affect the amount of lattice contraction, in addition to the amount and distribution of Cr secondary states in the bulk including Cr_2O_3 or metallic Cr [3,6]. Pertinent to the investigation, when the rate of lattice parameter contraction (Δa_{cr}) is considered, the present study provides the smallest values with -1.845×10^{-7} and -0.390×10^{-7} for absolute and normalised data respectively determined from line-of-best-fit fitting. The calculated Δa_{cr} for the present and described studies can be found in Table 2, which provides the line of best fit, $a = (\Delta a_{cr})x + a_o$, for the absolute and normalized data in this study and references. This stark difference in contraction can be readily observed in Fig. 2b with the shallowest line of best fit for the present investigation for both absolute and normalized lattice parameter data. The normalised Δa_{cr} for the present investigation is over 2-fold smaller than that of the nearest study of Leenaers et al. [10], who used conditions that only slightly better favour structure incorporation and enhanced lattice parameter contraction, a two-fold difference would not account for this [6]. It is previously understood that measurement of pellet samples can carry significant error and drift in acquired data [14], particularly if the heights of the samples are not properly calibrated relative to the source X-ray beam [15]. Further error is then found due common roughness of ceramic materials compared to thin-films or metallic samples [25]. Such effects may not significantly impact rudimentary sample measurement and data analysis, for example classical solid solutions, but when changes to the lattice parameter are

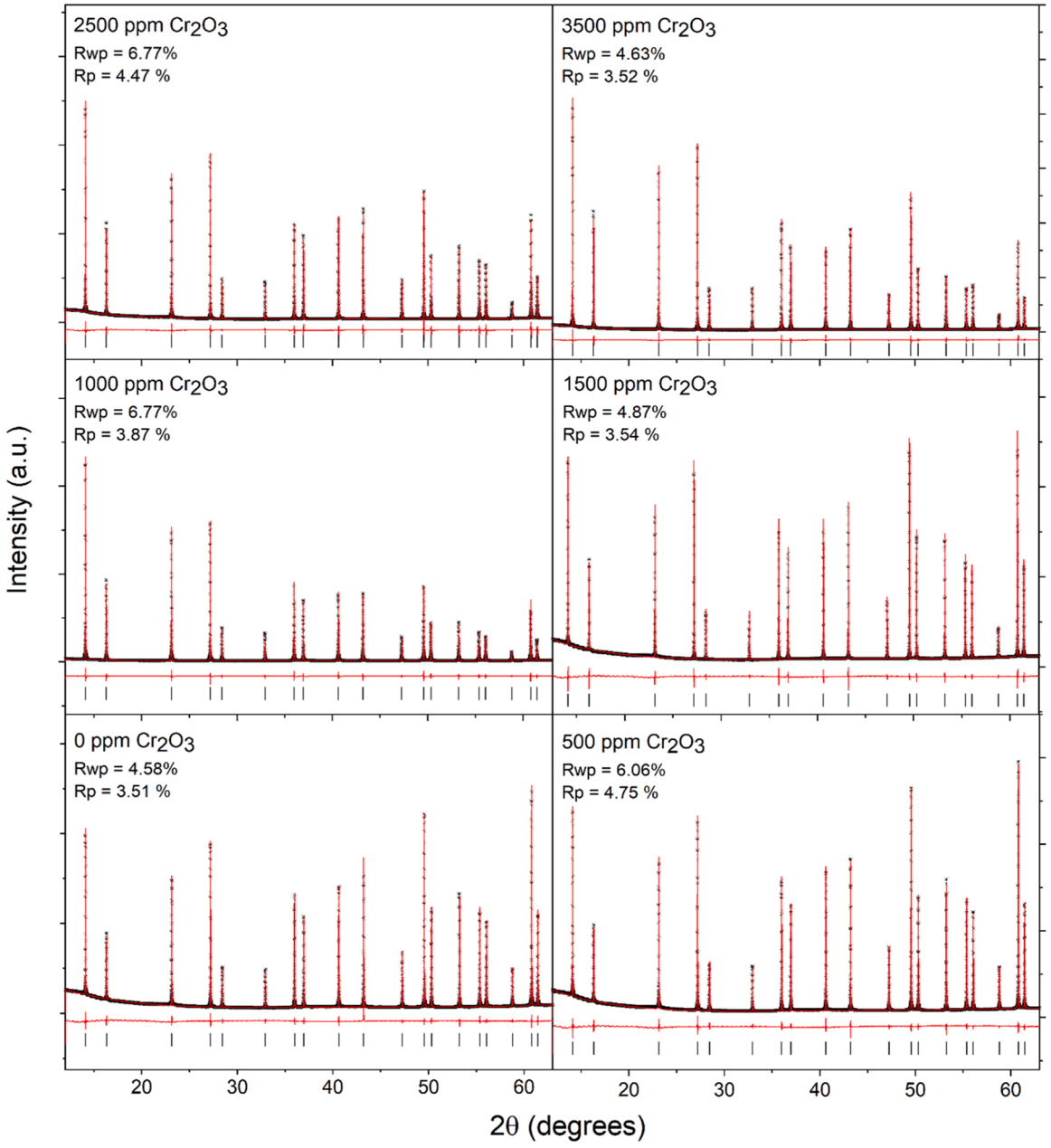

Fig. 1. Rietveld profiles made against S-XRD data collected on Cr-doped UO_2 powder samples with 0, 500, 1000, 1500, 2500 and 3500 ppm additions as Cr_2O_3 all recorded at 23 °C for $\lambda = 0.7749$ Å. All structures were refined using a fluorite model in space group $Fm\bar{3}m$. Aberrations in the background are due to merging of the datasets during image processing whereas differences in intensities are a result of different packing densities of capillaries.

Table 1
Refined structural parameters for Cr-doped UO_2 with 0, 500, 1000, 1500, 2500 and 3500 ppm as Cr_2O_3 addition from S-XRD data recorded at 23 °C with $\lambda = 0.7749$ Å. The structures were refined in cubic fluorite structures with space group $Fm\bar{3}m$.

Cr addition ppm (Cr_2O_3/Cr)	Lattice parameter (Å)
0/0	5.46894(2)
500/342	5.46872(2)
1000/684	5.46868(3)
1500/1026	5.46856(3)
2500/1711	5.46842(4)
3500/2395	5.46824(4)

on the order 0.1-0.01 % in the case of trace Cr doping in UO_2 they do become significant. A solution to the roughness issue can be achieved using a finely polished surface, however it is known that the polishing of ceramic surfaces may introduce material strain that can impact acquired data [26]. The use of a finely ground powder sample mounted in a capillary assists in negating these described challenges of pellet measurement, dramatically increasing measurement quality, and importantly, reliability. Notwithstanding, some errors can be encountered from capillaries relating to packing density which affects acquired diffraction intensity in addition to the use of fine powders which can be susceptible to enhanced oxidation, depending on the atmosphere used during preparation.

It is important to highlight that although conditions were used in the present investigation that should result in a maximum solubility of 750 ppm Cr [6], lattice parameter contraction is observed above this value in

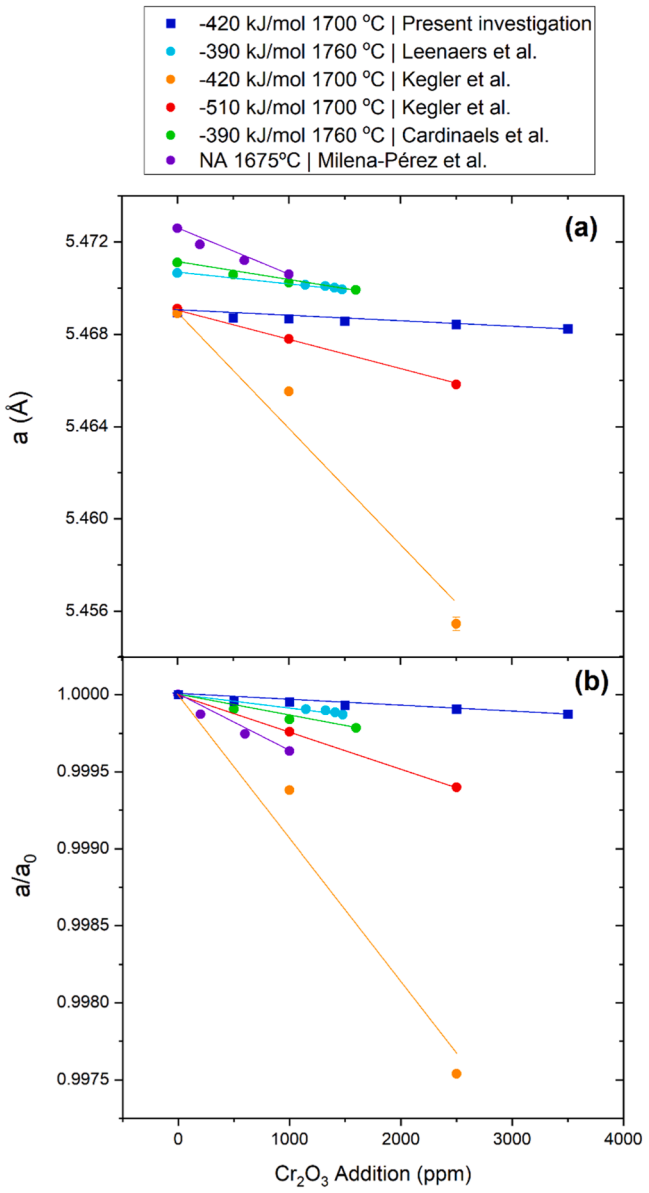

Fig. 2. (a) Absolute lattice parameter of Cr-doped UO_2 as a function of Cr doping (as Cr_2O_3 addition during synthesis) and (b) Normalized lattice parameter (a/a_o) for values determined from the present investigation via S-XRD measurements using fine powders and reference values from Leenaers et al. [10], Kegler et al. [7], Cardinaels et al. [11] and Milena-Pérez et al. [13]. The linear line-of-best-fits, $a = (\Delta a_{cr})x + a_o$, are provided, where x is the amount of Cr added as Cr_2O_3, Δa_{cr} is the rate of contraction, a_o is the initial lattice parameter and a is the determined lattice parameter. Determined values for the linear line-of-best-fit are provided in Table 2.

terms of amount of Cr added in synthesis. This is due to the distribution of Cr among the Cr bearing phases in bulk UO_2 including matrix incorporated $(Cr_x^{+3}U_{1-x}^{+4})O_{2-0.5x}$, and secondary metallic and oxide phases that occur across grain boundaries and as precipitates [3,4,6,27]. Additionally, the synthesis is consistently susceptible to volatilisation of Cr [8], further affecting the amount of actual Cr that enters the UO_2 lattice matrix. We previously showed [3] using high energy resolution fluorescence detection X-ray absorption near edge spectroscopy (HERFD-XANES) and quantifying using iterative transformation factor analysis (ITFA) for Cr-doped UO_2 with 3500 ppm addition Cr as Cr_2O_3 (2395 ppm as Cr) the Cr redox states in the bulk material can be accounted for as 65 % Cr^{+3}, 26 % Cr^{+2}, and 9 % Cr metallic. In which chemically these are attributed to lattice matrix $(Cr_x^{+3}U_{1-x}^{+4})O_{2-0.5x}$ (44 %), precipitate $Cr_2^{+3}O_3$ (21 %), grain boundary/sub-stoichiometric chromia Cr^{+2}, and metallic Cr^0. This phase assemblage distribution was found to match the thermodynamic model described for Cr-doped UO_2 by Riglet-Martial et al. [6]. When accounting for the volatility of Cr which reaches approximately 30 % [8], this results in 1677 ppm Cr (as Cr) to be distributed among these phases. Noting the solubility limit of Cr under synthesis conditions used, this results in a distribution of approximately 750 ppm for $(Cr_x^{+3}U_{1-x}^{+4})O_{2-0.5x}$, 340 ppm for $Cr_2^{+3}O_3$, 436 ppm for Cr^{+2} and 151 ppm for metallic Cr^0. If we then consider lower addition of Cr, for instance 2500 ppm Cr_2O_3 (1711 ppm as Cr), after 30 % volatilization this results in 1198 ppm of Cr (as Cr) for distribution among the phases. The thermodynamic model for consistent conditions implies a similar distribution of Cr phases resulting in 535 ppm Cr for $(Cr_x^{+3}U_{1-x}^{+4})O_{2-0.5x}$, 243 ppm Cr for $Cr_2^{+3}O_3$, 311 ppm for Cr^{+2} and 107 ppm for metallic Cr^0, hence the lattice structure is undersaturated with Cr and is less contracted relative to the sample prepared at 3500 ppm addition as Cr_2O_3. This described analysis pertinently carries errors particularly from the ITFA analysis with a known 5 % [28], but nevertheless guides the distribution of states and allows understanding of continual linear contraction of the UO_2 lattice at what could be considered high doping amounts of Cr. Accordingly, it is pertinent to highlight in this study and others that the addition of Cr does not correspond to the amount of Cr that enters the UO_2 lattice matrix and affects the lattice parameter, but depends on the conditions used during synthesis and associated distribution of Cr states [6]. Notably, direct determination of the Cr content in the UO_2 lattice matrix can be achieved using electron microprobe analysis (EPMA). However, EPMA has not been commonly used in Cr-doped UO_2 investigations in part due to its impressive cost of acquisition. Nevertheless, as shown in the present investigation and others, diffraction is a relatively inexpensive means of tracking the incorporation of Cr into UO_2.

The use of a synchrotron X-ray source for precise lattice determination is a pertinent component of this investigation. Synchrotron sources provide far superior measurement resolution which subsequently results in more precise and accurate structural data, in this instance the lattice parameter of UO_2 as Cr is incorporated into it. Consequently, we argue that the results of this investigation provide the highest precision and best describe the structural dependence of Cr incorporation into UO_2. Pertinently, we emphasis caution in the interpretation of data acquired from measurements intended for more rudimentary analysis, particularly on non-ideally prepared sample states. This is not to say such results are invalid, as they can readily guide and assist in the fabrication of Cr-doped UO_2 fuel bodies for material property research and application. However, in interpreting subtle atomic effects such as the degree to which the fluorite structure contracts based on the specific redox states that occur due to trace dopants, caution and insurance is needed via high resolution measurement and careful specimen preparation.

The lattice dependence of the UO_2 fluorite structure as a function of Cr doping with 0, 500, 1000, 1500, 2500 and 3500 ppm addition as Cr_2O_3 when prepared under conditions of 1700 °C and -420 kJ/mol has been established via Rietveld refinements against high resolution synchrotron X-ray powder diffraction data. The results obtained, which appear to be the first using a high-resolution X-ray measurement, indicate that the lattice parameter contraction is considerably lessened and much more subtle than previous investigations have shown. The enhanced lattice parameter values obtained in this investigation compared to previous are attributed to the accuracy and resolution of synchrotron measurements performed on fine powders mounted in capillaries compared to standard laboratory X-ray measurements often performed on pellets which can carry significantly higher uncertainty and potential error from incorrect preparation. Methods are available to correct against specific errors arising from certain sample types, however, care and consideration is required to ensure correct mitigation particularly when considering the desired property of a material to be measured and determined. Moreover, the investigation has provided critical guidance to previous varying descriptions of the Cr-doped UO_2

Table 2
Linear equations for line-of-best-fit for UO_2 fluorite lattice as a function of Cr_2O_3 addition, $a = (\Delta a_{cr})x + a_o$, for absolute and normalized lattice parameter data where x is the amount of Cr added as Cr_2O_3, Δa_{cr} is the rate of contraction, a_o is the initial lattice parameter and a the determined lattice parameter. Δa_{cr} is bolded for clarity.

Study and measurement type	Absolute linear line-of-best-fit	R^2	Normalised line-of-best-fit	R^2	Conditions (T/ μ_{O2})
Present Investigation S-XRD| Powder	$a = (\mathbf{-1.845\times10^{-7}})x + 5.4689$	0.967	$a = (\mathbf{-0.390\times10^{-7}})x + 1$	0.928	1700 °C/ -420 kJ/mol
Leenaers et al. [10]. XRD| Polished Pellet	$a = (\mathbf{-4.547\times10^{-7}})x + 5.4707$	0.989	$a = (\mathbf{-0.824\times10^{-7}})x + 1$	0.989	1760 °C/ -390 kJ/mol
Kegler et al. [7]. XRD| Pellet	$a = (\mathbf{-41.055\times10^{-7}})x + 5.4686$	0.956	$a = (\mathbf{-7.732\times10^{-7}})x + 1$	0.955	1700 °C/ -420 kJ/mol
Kegler et al. [7]. XRD| Pellet	$a = (\mathbf{-14.106\times10^{-7}})x + 5.4692$	0.983	$a = (\mathbf{-2.425\times10^{-7}})x + 1$	0.977	1700 °C/ -520 kJ/mol
Cardinaels et al. [11]. XRD| Polished Pellet	$a = (\mathbf{-8.014\times10^{-7}})x + 5.4711$	0.998	$a = (\mathbf{-1.511\times10^{-7}})x + 1$	0.977	1760 °C/ -390 kJ/mol
Milena-Pérez et al. [13]. XRD| Polished Pellet	$a = (\mathbf{-19.237\times10^{-7}})x + 5.4724$	0.972	$a = (\mathbf{-3.890\times10^{-7}})x + 1$	0.952	1675 °C/ NA

lattice parameter dependence, in which it highlights the importance of using high resolution diffraction methods to determine subtle changes precisely to crystal structures of ceramics when doped with trace elements and supports the scientific understanding of Cr-doped UO_2 nuclear fuels.

CRediT authorship contribution statement

Gabriel L. Murphy: Writing – review & editing, Writing – original draft, Supervision, Project administration, Methodology, Investigation, Funding acquisition, Formal analysis, Data curation, Conceptualization. **Volodymyr Svitlyk:** Writing – review & editing, Methodology, Formal analysis, Investigation. **Maximilian Henkes:** Writing – review & editing, Methodology, Investigation. **Daniil Shirokiy:** Writing – review & editing, Methodology, Formal analysis, Investigation. **Christoph Hennig:** Formal analysis, Investigation. **Philip Kegler:** Writing – review & editing, Methodology, Investigation. **Dirk Bosbach:** Writing – review & editing, Formal analysis, Methodology, Investigation. **Andrey Bukaemskiy:** Writing – review & editing, Methodology, Investigation, Formal analysis, Conceptualization.

Declaration of competing interest

The authors all declare they have no competing financial interests or potential relationships that could have appeared to influence the world to reported in this paper.

Data availability

Data will be made available on request.

Acknowledgments

The authors are grateful to funding and support from the German Federal Ministry of Education and Research (BMBF), Project No. 02NUK060 that enabled this research.

References

[1] J. Arborelius, K. Backman, L. Hallstadius, M. Limbaeck, J. Nilsson, B. Rebensdorff, G. Zhou, K. Kitano, R. Loefstroem, G. Roennberg, Advanced doped UO_2 pellets in LWR applications, J. Nucl. Sci. Technol. 43 (9) (2006) 967–976.
[2] J. Killeen, Fission gas release and swelling in UO_2 doped with Cr_2O_3, J. Nucl. Mater. 88 (2–3) (1980) 177–184.
[3] G.L. Murphy, R. Gericke, S. Gilson, E.F. Bazarkina, A. Rossberg, P. Kaden, R. Thümmler, M. Klinkenberg, M. Henkes, P. Kegler, V. Svitlyk, J. Marquardt, T. Lender, C. Hennig, K.O. Kvashnina, N. Huittinen, Deconvoluting Cr states in Cr-doped UO_2 nuclear fuels via bulk and single crystal spectroscopic studies, Nat. Commun. 14 (1) (2023) 2455.
[4] S.C. Middleburgh, S. Dumbill, A. Qaisar, I. Vatter, M. Owen, S. Vallely, D. Goddard, D. Eaves, M. Puide, M. Limbäck, Enrichment of chromium at grain boundaries in chromia doped UO_2, J. Nucl. Mater. 575 (2023) 154250–154254.
[5] A. Devillaire, L. Desgranges, N. Tarisien, X. Iltis, C. Riglet-Martial, I. Roure, P. Bienvenu, A. Canizares, Characterisation of 3000 ppm Cr_2O_3 doped UO_2 and its precipitates, J. Raman Spectrosc. 54 (2) (2023) 1–7.
[6] C. Riglet-Martial, P. Martin, D. Testemale, C. Sabathier-Devals, G. Carlot, P. Matheron, X. Iltis, U. Pasquet, C. Valot, C. Delafoy, Thermodynamics of chromium in UO_2 fuel: a solubility model, J. Nucl. Mater. 447 (1–3) (2014) 63–72.
[7] P. Kegler, M. Klinkenberg, A. Bukaemskiy, G.L. Murphy, G. Deissmann, F. Brandt, D. Bosbach, Chromium doped UO_2-based ceramics: synthesis and characterization of model materials for modern nuclear fuels, Materials 14 (20) (2021) 6160–6178 (Basel).
[8] V. Peres, L. Favergeon, M. Andrieu, J.C. Palussière, J. Balland, C. Delafoy, M. Pijolat, High temperature chromium volatilization from Cr_2O_3 powder and Cr_2O_3-doped UO_2 pellets in reducing atmospheres, J. Nucl. Mater. 423 (1) (2012) 93–101.
[9] M.W.D. Cooper, C.R. Stanek, D.A. Andersson, The role of dopant charge state on defect chemistry and grain growth of doped UO_2, Acta Mater. 150 (2018) 403–413.
[10] A. Leenaers, L. de Tollenaere, C. Delafoy, S. Van den Berghe, On the solubility of chromium sesquioxide in uranium dioxide fuel, J. Nucl. Mater. 317 (1) (2003) 62–68.
[11] T. Cardinaels, K. Govers, B. Vos, S. Van den Berghe, M. Verwerft, L. de Tollenaere, G. Maier, C. Delafoy, Chromia doped Uo_2 fuel: investigation of the lattice parameter, J. Nucl. Mater. 424 (1) (2012) 252–260.
[12] M. Sun, J. Stackhouse, P.M. Kowalski, The+ 2 oxidation state of Cr incorporated into the crystal lattice of UO_2, Commun. Mater. 1 (1) (2020) 1–8.
[13] A. Milena-Pérez, L.J. Bonales, N. Rodríguez-Villagra, S. Fernández, V.G. Baonza, J. Cobos, Raman spectroscopy coupled to principal component analysis for studying UO_2 nuclear fuels with different grain sizes due to the chromia addition, J. Nucl. Mater. 543 (2021) 152581–152592.
[14] X. Chen, S. Bates, K.R. Morris, Quantifying amorphous content of lactose using parallel beam X-ray powder diffraction and whole pattern fitting, J. Pharm. Biomed. Anal. 26 (1) (2001) 63–72.
[15] G. Baldinozzi, D. Simeone, J.F. Bérar, S. Bouffard, Y. Zhang, Glancing incidence diffraction as a non-destructive tool to improve functional and structural systems for future nuclear applications. Materials, Processing, and Characterization Techniques for Future Nuclear Technologies, Warsaw, Poland, 2014.
[16] G.L. Murphy, Z. Zhang, R. Tesch, P.M. Kowalski, M. Avdeev, E.Y. Kuo, D.J. Gregg, P. Kegler, E.V. Alekseev, B.J. Kennedy, Tilting and distortion in rutile-related mixed metal ternary uranium oxides: a structural, spectroscopic, and theoretical investigation, Inorg. Chem. 60 (4) (2021) 2246–2260.
[17] G.L. Murphy, C.H. Wang, Z.M. Zhang, P.M. Kowalski, G. Beridze, M. Avdeev, O. Muransky, H.E.A. Brand, Q.F. Gu, B.J. Kennedy, Controlling oxygen defect formation and its effect on reversible symmetry lowering and disorder-to-order phase transformations in nonstoichiometric ternary uranium oxides, Inorg. Chem. 58 (9) (2019) 6143–6154.
[18] G.L. Murphy, B.J. Kennedy, Z. Zhang, M. Avdeev, H.E.A. Brand, P. Kegler, E. V. Alekseev, Structure and phase transition in $BaThO_3$: a combined neutron and synchrotron X-ray diffraction study, J. Alloy. Compd. 727 (2017) 1044–1049.
[19] G.L. Murphy, B.J. Kennedy, J.A. Kimpton, Q. Gu, B. Johannessen, G. Beridze, P. M. Kowalski, D. Bosbach, M. Avdeev, Z. Zhang, Nonstoichiometry in strontium uranium oxide: understanding the rhombohedral–orthorhombic transition in $SrUO_4$, Inorg. Chem. 55 (18) (2016) 9329–9334.
[20] A.C. Scheinost, J. Claussner, J. Exner, M. Feig, S. Findeisen, C. Hennig, K. O. Kvashnina, D. Naudet, D. Prieur, A. Rossberg, M. Schmidt, C. Qiu, P. Colomp, C. Cohen, E. Dettona, V. Dyadkin, T. Stumpf, ROBL-II At Esrf: a synchrotron toolbox for actinide research, J. Synchrotron Radiat. 28 (1) (2021) 333–349.
[21] J. Kieffer, V. Valls, N. Blanc, C. Hennig, New tools for calibrating diffraction setups, J. Synchrotron Radiat. 27 (2) (2020) 558–566.
[22] B.H. Toby, R.B. Von Dreele, GSAS-II: the genesis of a modern open-source all purpose crystallography software package, J. Appl. Crystallogr. 46 (2) (2013) 544–549.
[23] G. Leinders, T. Cardinaels, K. Binnemans, M. Verwerft, Accurate lattice parameter measurements of stoichiometric uranium dioxide, J. Nucl. Mater. 459 (2015) 135–142.
[24] G.L. Murphy, Z. Zhang, H.E. Maynard-Casely, J. Stackhouse, P.M. Kowalski, T. Vogt, E.V. Alekseev, B.J. Kennedy, Pressure induced reduction in $SrUO_4$ – A

topotactic pathway to accessing extreme incompressibility, Acta Mater. 243 (2023) 118508.
[25] R.P. Goehner, M.O. Eatough, A study of grazing incidence configurations and their effect on X-ray diffraction data, Powder Diffr. 7 (1) (1992) 2–5.
[26] V. Darakchieva, B. Monemar, A. Usui, On the lattice parameters of GaN, Appl. Phys. Lett. 91 (3) (2007) 031911–031913.
[27] P. Seo, K. Yasuda, S. Matsumura, N. Ishikawa, G. Gutierrez, J.M. Costantini, Microstructure evolution in 200-MeV Xe ion irradiated CeO_2 doped with Gd_2O_3, J. Appl. Phys. 132 (23) (2022) 2359021–23590213.
[28] A. Rossberg, T. Reich, G. Bernhard, Complexation of uranium (Vi) with protocatechuic acid—application of iterative transformation factor analysis to EXAFS spectroscopy, Anal. Bioanal. Chem. 376 (5) (2003) 631–638.